Available online at www.sciencedirect.com

SCIENCE DIRECT®

Journal of Photochemistry and Photobiology A: Chemistry 169 (2005) 177–185

Journal of Photochemistry and Photobiology A:Chemistry

www.elsevier.com/locate/jphotochem

Effect of UV radiation on the semi-interpenetrating polymer networks based on polyurethane and epoxy maleate of bisphenol A

L. Rosu [a], C.N. Cascaval [a,*], C. Ciobanu [a], D. Rosu [a], E.D. Ion [b], C. Morosanu [b], M. Enachescu [c]

[a] *Department of Polymeric Materials, "Petru Poni" Institute of Macromolecular Chemistry, Romanian Academy Alley Gr. Ghica Voda, 41A, Iassy 700487, Romania*
[b] *National Institute for Material Physics, P.O. Box MG-7, Bucharest-Magurele, Romania*
[c] *Lawrence Berkeley National Laboratory, University of California, Berkeley, CA 94720, USA*

Received 11 May 2004; accepted 8 June 2004
Available online 5 August 2004

Abstract

The behavior of two semi-interpenetrating polymer networks (S-IPNs) based on polyurethane (PU) and epoxy maleate of bisphenol A (EMBA) under exposure to UV radiation for long period of times (up to 200 h) was investigated. The networks obtained by the specific mixture under certain thermal treatment included in their structures crosslinked EMBA and linear PU. Advanced photooxidative degradation took place for long time of UV irradiation (over 160 h, especially), with almost a total destruction of the raw structures. The important modification of both the surface and of the morphology of the tested samples with the time of irradiation was also analyzed. Simultaneously, as compared to results obtained for short time of UV radiations (up to 10 h), where the mechanical properties of the tested samples improved, long time of UV radiations led to deterioration of many of the mechanical properties.

Keywords: UV radiation; Polyurethane; Epoxy maleate; Networks; Photooxidative degradation

1. Introduction

Because of its high tensile strength, chemical resistance, good processability and mechanical properties, polyurethane (PU) is being used in many technical applications [1]. Both PU and compositions-based PU are widely used as protection films and/or agents for modification of the surface properties of various materials. The most important compositions of PU intended to be used as protection films are interpenetrating polymer networks (IPNs) and semi-interpenetrating polymer networks (S-IPNs) [2–5].

Although the materials with urethane structures exhibit good mechanical properties their use as surface coatings in outdoor applications is limited by the sensibility to the photooxidative degradation, which can lead to the discoloration and even the total destruction.

Experimental studies, carried out previously [4–6], showed that the photooxidation of the aromatic diisocyanate PUs proceeds by a complex mechanism. A great number of factors influences the photooxidative degradation of PU, such as macromolecular and supramolecular structure, the physical state of the polymer (film, solution, etc.), the irradiation conditions, as well as the presence or absence of the oxygen in the environment during irradiation.

Although IPNs based PU were the subject of many studies [7–10], these polymeric materials were less investigated regarding their behavior to the UV radiations. In our previous works, PU-epoxy maleate of bisphenol A (EMBA) blends [11], as well as, PU-EMBA S-IPNs [12] were synthesized and characterized according to their miscibility and to the thermal behavior [13]. The synthesized S-IPNs showed a high degree of miscibility and good thermal properties. The change of the mechanical properties induced by irradiation with duration up to 200 h was also studied. Under UV radiation of less than 10 h, the mechanical properties of the tested S-IPNs were greatly, improved. This behavior was associated with a high and permanent interpenetrating of the PU and EMBA polymers in the networks due to some additional crosslinks generated by UV radiation. However, under much higher UV irradiation exposure, e.g. 160 h, a sensible deterioration of the mechanical properties was observed.

---

[*] Corresponding author. Tel.: +40-232-217454; fax: +40-232-211299.
E-mail address: cascaval@icmpp.tuiasi.ro (C.N. Cascaval).

1010-6030/$ – see front matter © 2004 Elsevier B.V. All rights reserved.
doi:10.1016/j.jphotochem.2004.06.008

The aim of this work is to present the modifications of both structural, morphological and the physico-mechanical properties of PU-EMBA S-IPNs as a consequence of exposure to UV radiation for a long period of time.

2. Experimental

2.1. Materials

PU used in this study was synthesized by fusion condensation of adipic acid, ethylene glycol and diethylene glycol (1:0.5:0.6 molar ratio) with 4,4′-diphenylmethane diisocyanate (MDI), as was previously reported [14]. EMBA resin was obtained using maleic anhydride, Dinox epoxy resin and water [11]. Dinox resin was a commercial product prepared from bisphenol A in reaction with epichlorohydrin. PU-EMBA S-IPNs were prepared after a sequential procedure by mixing PU and EMBA solutions in dimethylformamide (DMF), in presence of benzoyl peroxide [12]. The mixture were cast on glass slides and subsequently soft baked at 120 °C for 3 h on a hot plate. EMBA resin crosslinked and contained the linear PU in its network structure. Two S-IPNs were synthesized, the first one (S-IPN-1) with low EMBA content (11.11 wt.%) and the second one (S-IPN-2) with 27.3 wt.% EMBA.

2.2. Irradiation and analysis

The UV irradiation of the synthesized S-IPNs was carried out by means of a middle-pressure mercury lamp, HQE-40 type, having a polychrome emission spectrum, in the presence of air. The more energetic radiation (not presented in the natural light) was eliminated using a 30 μm borosilicate glass filter. The samples, as films, were mounted on a rotative device, which was positioned at a distance of 60 mm from the lamp. Using a fan, the temperature inside the irradiation chamber was kept at 45 °C.

The IR spectra were obtained at a nominal resolution of 2 cm^{-1} on an M80 Specord spectrophotometer using KBr pellets.

The optical microscopy (OM) micrographs were obtained with a MC5A (300×) optical microscope (IOR-Bucharest, Romania).

The atomic force microscopy (AFM) measurements were performed at the NANOTECH-21 laboratory [15], using a custom-built digital signal processor controlled system [16], capable of atomic resolution on mica and graphite under environmental conditions. AFM topographic images of the same surface were recorded over a scan area varying from 10 μm × 10 μm up to 37 μm × 37 μm, each image having a resolution of 256 × 256 data points. In order to quantitatively investigate the topography of the samples, a study of the roughness distribution for a very large set of data, involving parameters like root-mean-square (RMS) roughness, was performed.

The physico-mechanical measurements were carried out by means of TIRA-TEST 2161 apparatus, at a crosshead speed of 20 mm/min.

3. Results and discussion

The IR spectra of the synthesized S-IPNs were very similar with that of the crude PU. Table 1 summarizes the most representative IR bands of both PU and of the two synthesized S-IPNs.

During irradiation the systematic changes in the IR spectra of the tested samples were noticed. The change of the absorbances in the IR spectra recorded for both PU and one of the synthesized S-IPNs (S-IPN-2) can be seen in Figs. 1 and 2, where the IR spectra of nonoirradiated samples (A), irradiated samples for 40 h (B), and the difference A−B (C) are presented.

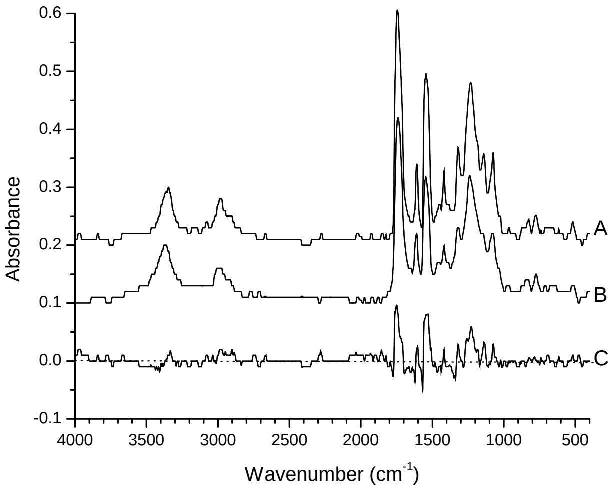

Fig. 1. IR spectra of PU: (A) nonirradiated sample; (B) irradiated sample 40 h; (C) difference A−B.

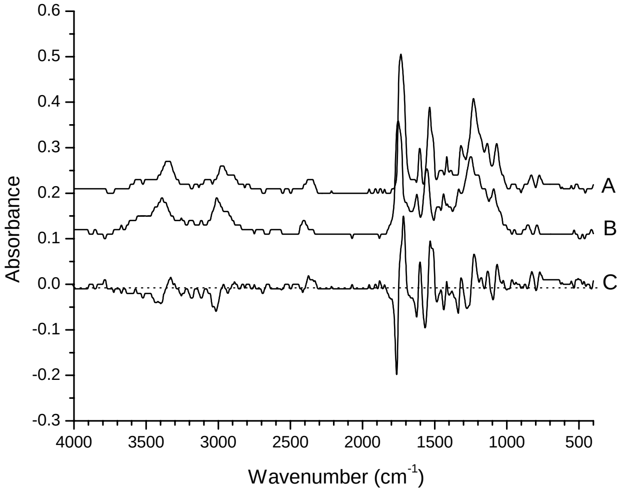

Fig. 2. IR spectra of S-IPN-2: (A) nonirradiated sample; (B) irradiated sample 40 h; (C) difference A−B.

Table 1
IR characteristics bands of PU, S-IPN-1 and S-IPN-2

PU frequency (cm^{-1})	S-IPN-1 frequency (cm^{-1})	S-IPN-2 frequency (cm^{-1})	Relative intensity[a]	Main assignment[b]
3369	3341	3359	m	$\nu_{N–H}$, associated
2996, 2938	2976	2893	m, sh	δ_{CH}, ν_{CH_2} in aromatic ring
1745	1735	1745	vs	$\nu_{C=O}$ in ester
1624	1606	1614	sh	$\nu_{C=O}$, associated in urethane
1594	1531	1542	vs	$\nu_{C–N} + \delta_{N–H}$, amide II
1484	1456	1466	w	δ_{CH_2}
1335	1317	1325	m	$\delta_{N–H} + \nu_{C–N}$, amide III
1242	1242	1252	s	$\nu_{C–O–C}$, in ester
1166	1138	1138	m	$\nu_{C–O–C}$, in ester
1083	1065	1065	m	$\nu_{C–O–C}$, in ester
832	813	831	w	$\nu_{C–H}$ in aromatic ring

[a] w: weak, m: medium, s: strong, vs: very strong, sh: shoulder.
[b] ν: stretching, δ: bending.

It is seen that several bands in the IR difference spectra C have negative and positive intensities. The negative absorbances reflect the structures that were formed during the UV irradiation, while the positive absorbances mark those structures that were lost.

The different spectrums show a strong decrease of the bands corresponding to the stretching vibration of N–H group (3359 cm^{-1}) and amide II (1528 cm^{-1}). Figs. 1 and 2 also display a decrease of the band at 1745 cm^{-1} (carbonyl stretching vibration in ester) and appearance of a new type of the carbonyl group at 1626 cm^{-1}, which is specific to some amidic structures.

Long-term UV irradiation of both PU and SIPNs led to a continuous decrease of the bands which were recorded for the nonirradiated samples. Figs. 3–5 show the IR spectra C of the tested samples obtained after 120, 160 and 200 h UV irradiation, respectively.

The samples UV treated for 120 h show many positive absorbances and less negative absorbances. PU UV treated

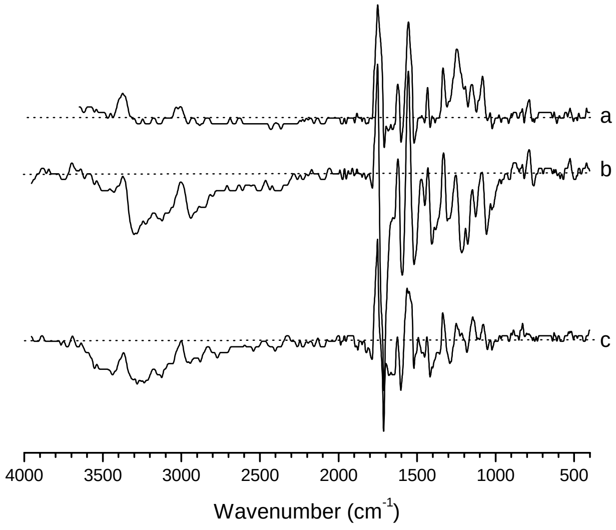

Fig. 3. IR difference spectra of PU obtained after: (a) 120 h; (b) 160 h; (c) 200 h UV irradiation time.

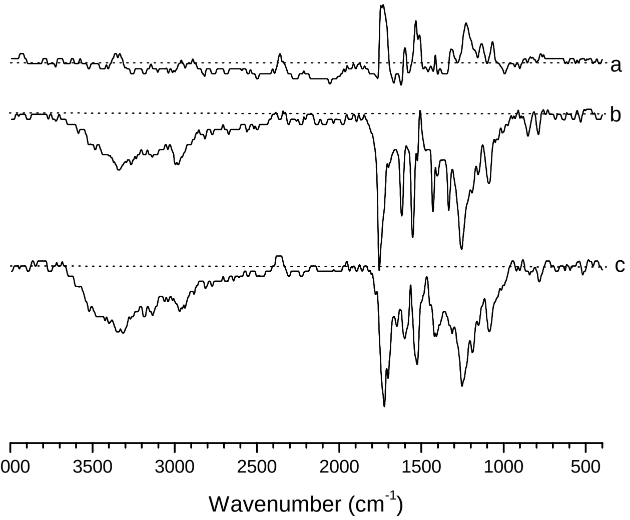

Fig. 4. IR difference spectra of S-IPN-1 obtained after: (a) 120 h; (b) 160 h; (c) 200 h irradiation time.

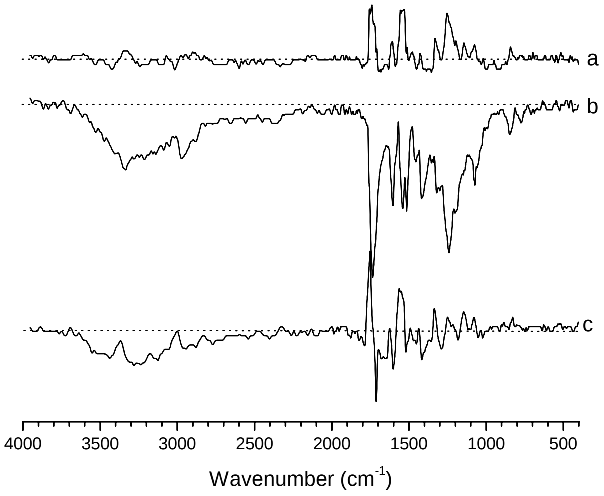

Fig. 5. IR difference spectra of S-IPN-2 obtained after: (a) 120 h; (b) 160 h; (c) 200 h irradiation time.

for 160 h, along with the structures which were put in evidence at 40 h UV irradiation, shows very few positive peaks and much more negative peaks. At this time of irradiation the synthesized S-IPNs show mainly negative peaks, suggesting a high density of new structures that were formed during UV irradiation. The new bands at 1594, 788 and 755 cm^{-1} correspond to the aromatic structures, those from 1717 cm^{-1} are specific to the carbonyl group from the esteric structures, while the bands at 1740 cm^{-1} can be assigned to the carbonyl group from the urethane bond. A very advanced photooxidative degradation takes place at 200 h irradiation, when both PU and the synthesized S-IPNs show only the negative bands in the IR spectra C.

The decrease of the intensity of the bands with the duration of irradiation could be due to the presence of some photooxidative radicalic processes [17], which are responsible for the gradual yellowing and even the total destruction of the initial structures. The main decrease of the bands intensity can be associated with the loss of the urethane structures during UV irradiation. It is well known that in the PU structures oxygen attack CH_2 groups in the aliphatic diol part, with hydroperoxides formation [6]. The hydroperoxides decompose relatively fast and form carbonyls, as was evidenced by IR. The carbonyl formation will contribute to the increase of the mass (Fig. 6).

The curves in Fig. 6 show a continuous and a gentle increase of the PU mass in the first 100 h irradiation, due to the participation the oxygen from air to generate the hydroperoxides. This behavior is not so visible for S-IPN-1, as well as S-IPN-2, especially. As result of the instability of the hydroperoxides their fragmentation leads to products with low molecular weight and high volatility. A drastic decrease of the mass of the samples takes place after 80 h irradiation.

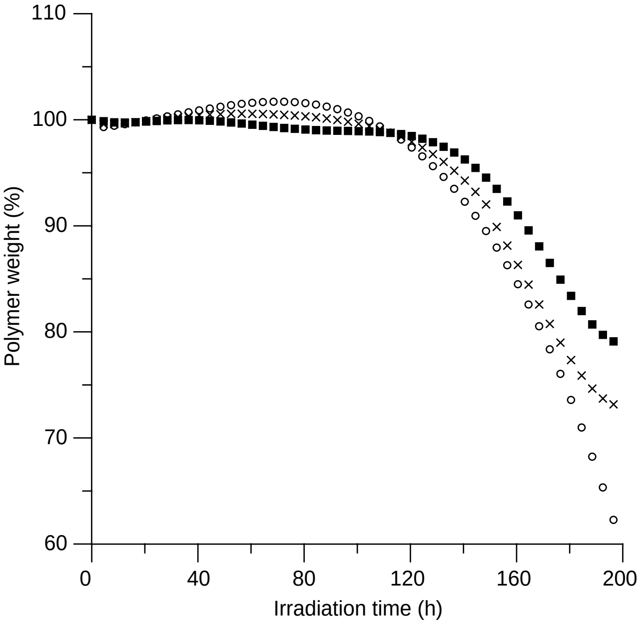

Fig. 6. Weight change of both PU and the tested S-IPNs vs. the irradiation time: (○) PU; (×) S-IPN-1; (■) S-IPN-2.

OM and AFM experimental techniques used in this study showed that UV radiation leads to important modifications in both surface and the morphology of PU, as well as of the tested S-IPNs. Fig. 7a–c, shows the OM micrographs of the networks surface, unexposed and exposed to UV radiations for various durations of time.

The samples before irradiation show a morphology with aspect of network [12], better outlined for S-IPN-2, especially. The unexposed samples have small pinholes of 0.1–2.0 μm diameter. When the films are exposed to UV radiation large holes appear. The appearance of wrinkles and micro-cracks on the film surface, in the presence of UV radiation, depends on the time of irradiation. As irradiation time increases, deterioration of surface becomes more visible, due to the accumulation of the volatile degradation products in the system.

To find further information regarding the morphology of the tested samples, the AFM technique was used to evaluate the RMS roughness, in order to obtain quantitative and qualitative analyses. Some AFM images of the network films, unexposed and exposed to UV radiations, for various periods of time, are shown in Fig. 8a–c.

The calculation of roughness was carried out for a great number of the experimental data, which were obtained for various irradiation times. The RMS roughness was calculated using the formula (1):

$$\mathrm{RMS} = \sum_{i=1}^{N} \left[\frac{(h_i - \bar{h})^2}{N} \right]^{1/2} \qquad (1)$$

where h_i represents the height value at each data point, $\bar{h}$ the profile mean value of the surface and N means the numbers of data points in the analyzed profile.

The roughness measured versus the irradiation time is shown in Fig. 9.

It was remarked for the tested samples a general decrease of the RMS values with the time of irradiation. The non-irradiated samples showed RMS values of 8 nm for PU, 243.5 nm for S-IPN-1 and 273 nm for S-IPN-2, while the samples which were irradiated 200 h presented the RMS values as follows: 22.4 nm for PU, 49.07 nm for S-IPN-1 and 57.66 nm for S-IPN-2, respectively. The small local maxima of RMS roughness registered for all the tested samples at 160 h confirm the data obtained by IR spectroscopy, namely, an advanced transformation of structures takes place for this irradiation time.

The change of the mechanical properties of the tested samples induced by UV radiations was also studied. Figs. 10 and 11 show the stress–strain curves recorded for both S-IPN-1 and S-IPN-2 samples using various irradiation times, while Table 2 lists some mechanical properties determined for PU and the synthesized S-IPNs.

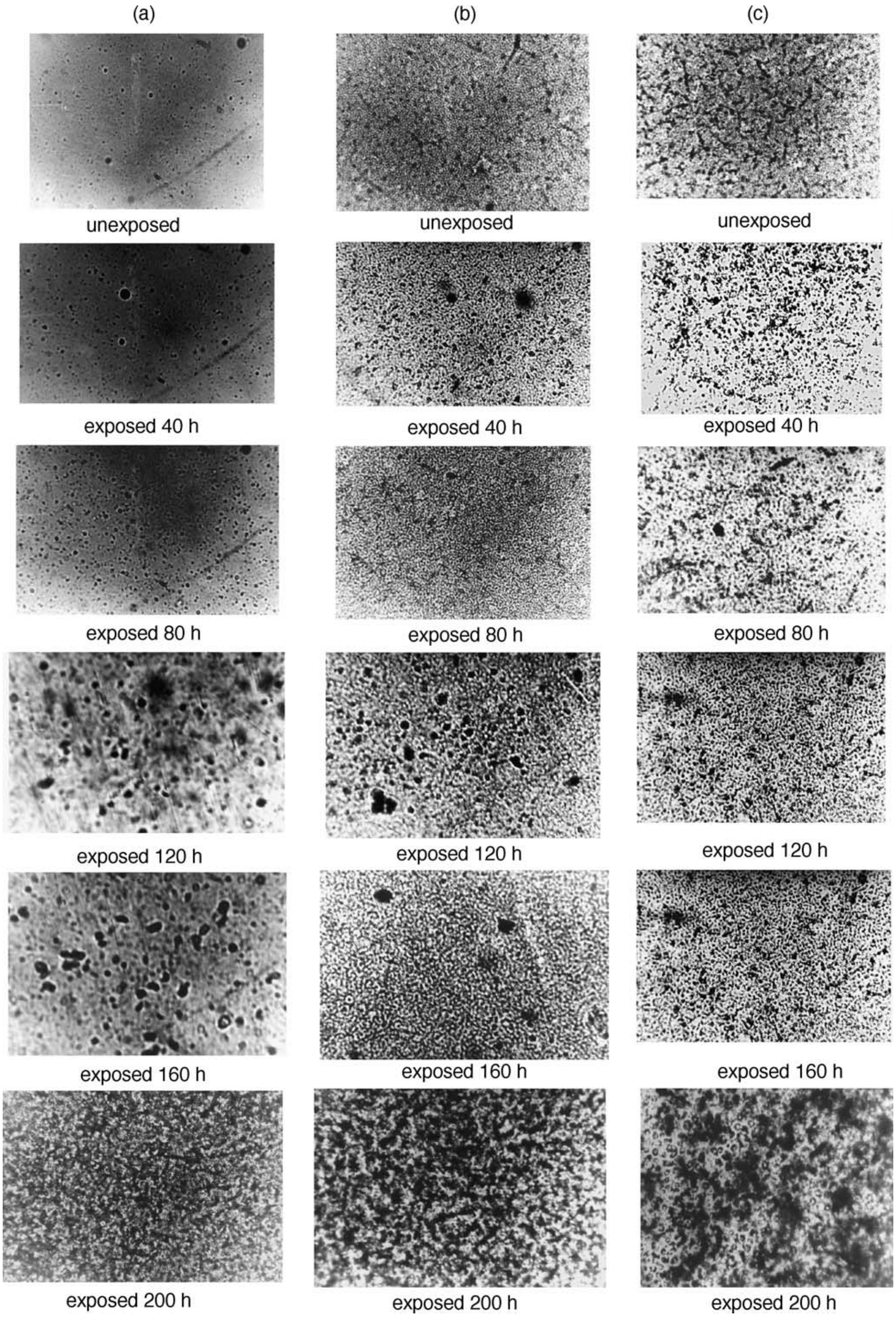

Fig. 7. OM micrographs (300×) of PU (a), S-IPN-1 (b) and S-IPN-2 (c).

It can be noted that the stress necessary for the strain of the same unit length for S-IPN-1 is higher as compared to that evaluated for S-IPN-2. Moreover, data listed in Table 2, with some inversions (for 160 h irradiation time, especially), show that the increase of the irradiation time leads to a pronounced increase of the initial modulus of elasticity for both PU and the two S-IPNs, and a moderate increase of the resistance at the limit of elasticity, as well as of the resistance at the break. The strain at the break shows a peculiar behavior. Generally, for PU, the strain at the break decreases with the increase of the irradiation time, while both S-IPN-1 and S-IPN-2 show an increase of the strain at

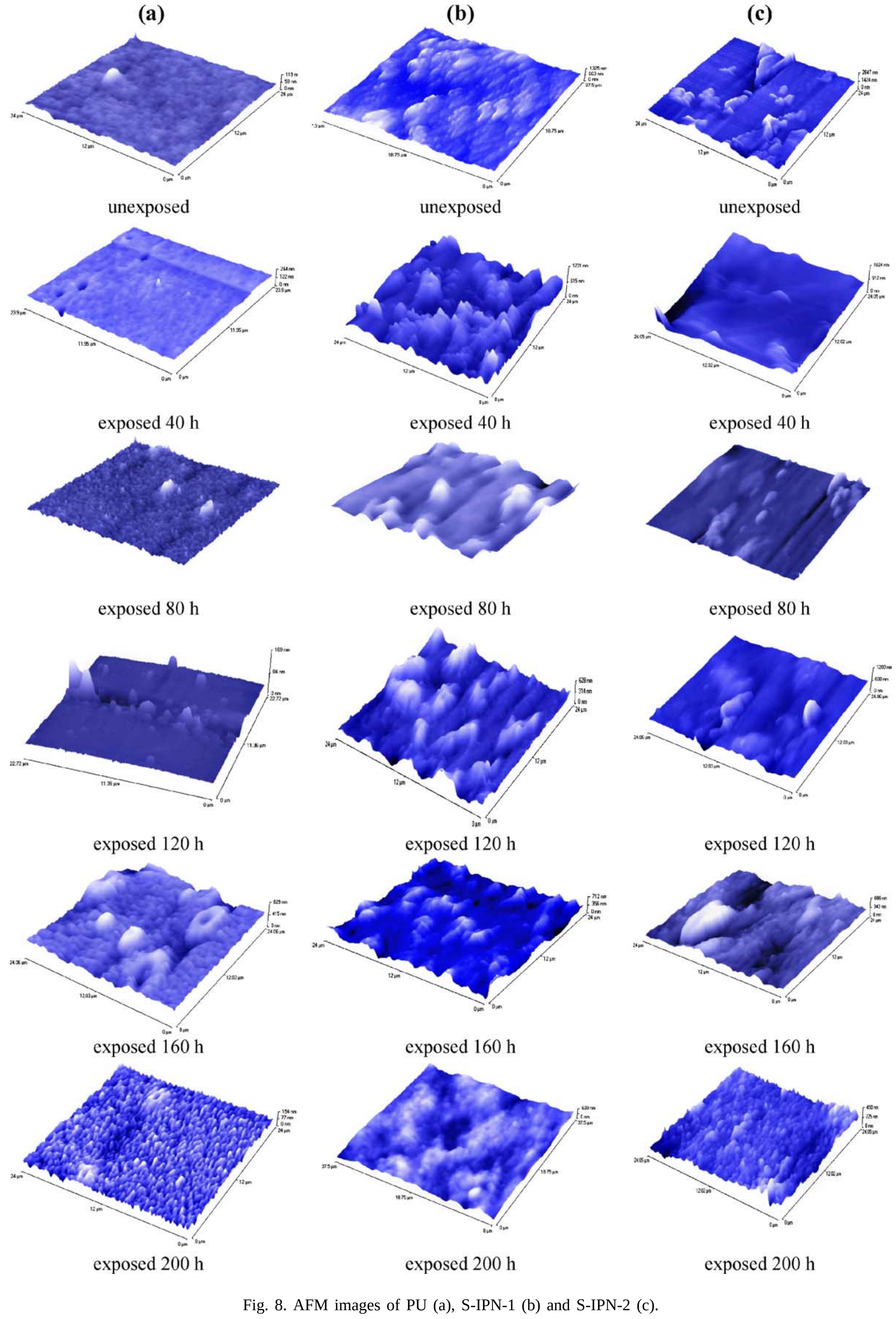

Fig. 8. AFM images of PU (a), S-IPN-1 (b) and S-IPN-2 (c).

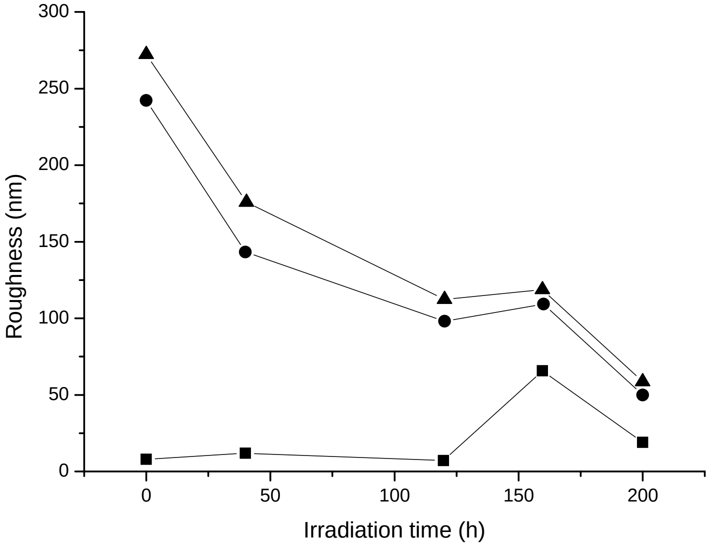

Fig. 9. Roughness measured vs. the irradiation time for PU (■), S-IPN-1 (●) and S-IPN-2 (▲).

the break for irradiation times up to 80 h, and than its values decrease.

As a general observation, the mechanical properties of both PU and of its interpenetrating networks with EMBA are much improved when the samples are exposed to UV radiations for durations up to 10 h [13]. Long times of irradiation leads to a moderate increase of some of the mechanical properties, associated with deterioration of others.

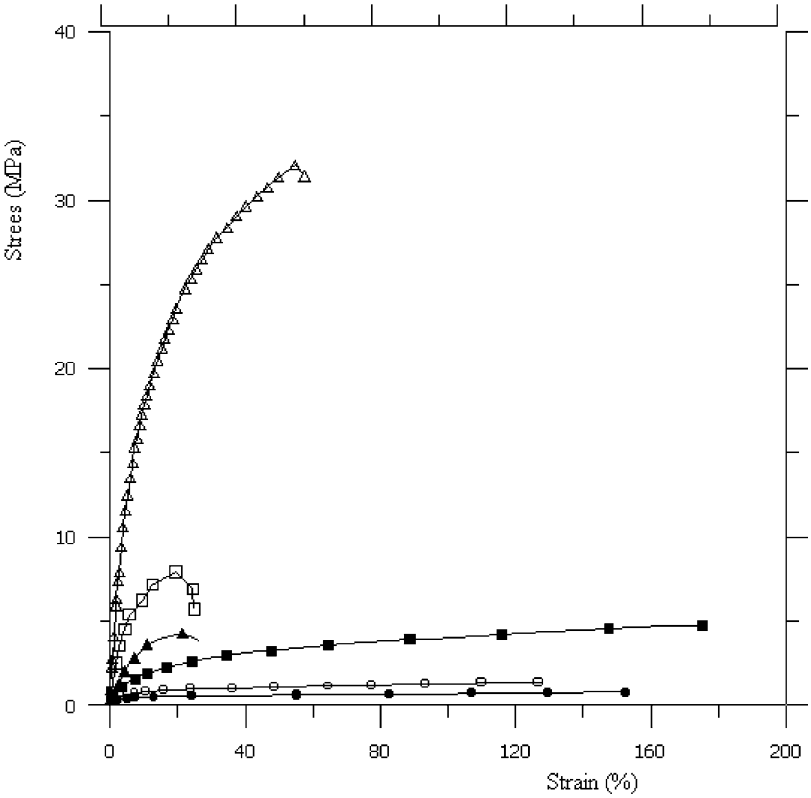

Fig. 10. Stress–strain curves for S-IPN-1: (●) unexposed; (○) exposed 40 h; (■) exposed 80 h; (□) exposed 120 h; (▲) exposed 160 h; (△) exposed 200 h.

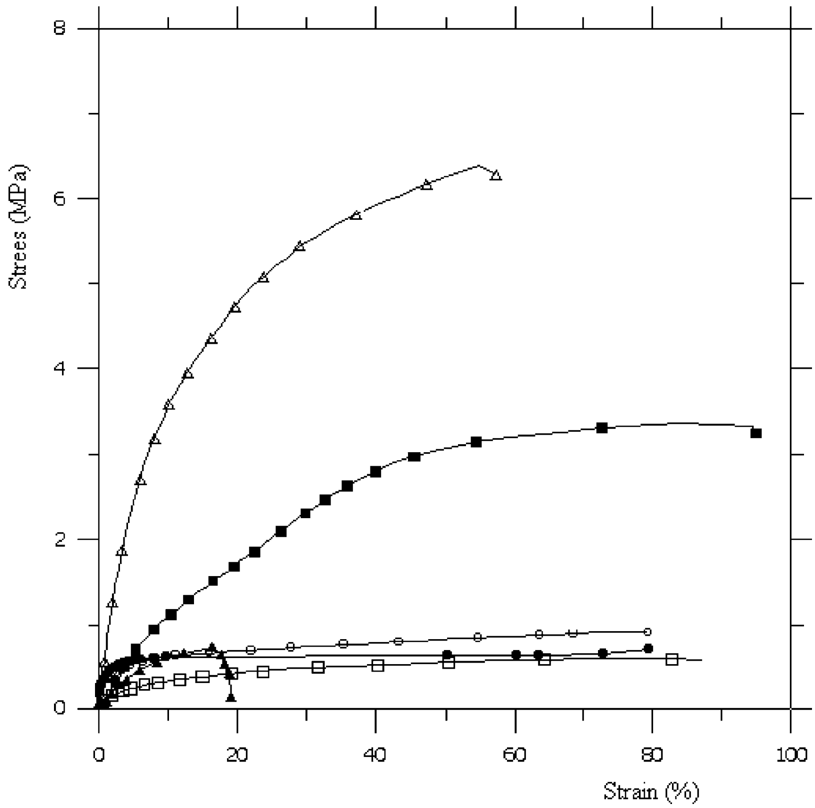

Fig. 11. Stress–strain curves for S-IPN-2: (●) unexposed; (○) exposed 40 h; (■) exposed 80 h; (□) exposed 120 h; (▲) exposed 160 h; (△) exposed 200 h.

Table 2
Physico-mechanical properties of the tested S-IPNs vs. the irradiation time

Sample	Time of irradiation (h)	Initial modulus of elasticity (MPa)	Resistance at the limit of elasticity (MPa)	Elongation at the *l* limit of elasticity (%)	Strain at the break (%)	Resistance at the break (MPa)
PU	0	4.7	0.5	6.0	261.0	1.8
	40	132.5	2.2	5.7	134.2	33.0
	80	190.7	15.7	5.4	180.5	52.7
	120	214.3	16.9	4.1	129.9	47.7
	160	225.7	15.4	5.4	117.0	46.4
	200	231.5	15.2	5.1	156.8	54.7
S-IPN-1	0	3.8	0.3	4.5	148.6	0.7
	40	14.0	0.5	2.2	122.3	1.3
	80	17.7	1.2	4.3	171.1	4.7
	120	86.2	5.3	5.6	19.3	7.9
	160	52.2	2.0	4.1	21.3	4.2
	200	444.4	4.7	6.4	54.8	32.0
S-IPN-2	0	12.0	0.5	1.5	63.7	0.6
	40	13.2	0.8	1.1	66.0	2.8
	80	14.7	15.7	3.9	85.5	3.3
	120	35.5	15.9	4.4	79.0	0.6
	160	11.0	15.4	2.8	16.3	0.7
	200	62.4	15.2	2.2	55.1	6.3

4. Conclusions

Two S-IPNs based on PU and EMBA were prepared in DMF and exposed to UV radiation for a duration up to 200 h. The results of this study showed that the UV radiations involved important modifications in the IR spectra of both PU and of the two synthesized PU-EMBA S-IPNs against the irradiation time.

Long-term UV irradiation led to a continuous decrease of the main bands intensity. A strong decrease of the bands corresponding to the stretching vibration of N–H groups (3359 cm^{-1}) and amide II (1528 cm^{-1}) was remarked at 40 h irradiation time. Starting with 160 h of UV irradiation an advanced photooxidative degradation takes place, with almost total destruction of the initial structures.

OM and AFM experiments showed that UV radiations provoked important modification in both surface and morphology of the tested samples. It was noted the formation of micro-cracks on the film surface. Deterioration of the surface become more visible as the time of irradiation increased. Simultaneously, for the tested samples, it was remarked a decrease of the RMS roughness with the irradiation time, even a local maxim was observed for 160 h UV irradiation.

As compared to results obtained with short UV irradiation time (up to 10 h) [13], PU and PU-EMBA S-IPNs exposed to long time of irradiation (up to 200 h) showed a moderate increase of some from their initial mechanical properties, with a great deterioration of others.

References

[1] J.H. Saunders, K.C. Frisch, Polyurethane Chemistry and Technology. Part I. Chemistry, Wiley, New York, 1962.
[2] L.H. Sperling, Interpenetrating Polymer Networks and Related Materials, Plenum Press, New York, 1981.
[3] D. Klempner, L.H. Sperling, L.A. Utraki, Interpenetrating Polymer Networks, American Chemical Society, Washington, DC, 1994.
[4] C. Wilhelm, J.L. Gardette, Polymer 38 (1997) 4019–4031.
[5] L. Irusta, M.J. Fernandez-Berridi, Polym. Deg. Stab. 63 (1999) 113–119.
[6] J.L. Gardette, J.J. Lemaire, Makromol. Chem. 182 (1981) 2723–2734.
[7] Y. Zhang, R.J. Heath, D.J. Hourston, J. Appl. Polym. Sci. 75 (2000) 406–416.
[8] D.J. Hourtson, J.A. McCluskie, J. Appl. Polym. Sci. 31 (1986) 645–655.
[9] S.R. Jin, J.M. Widmaier, G.C. Meyer, Polymer 29 (1998) 346–350.
[10] C.-H. Chen, W.-J. Chen, M.-H. Chen, Y.-M. Li, Polymer 41 (2000) 7961–7967.
[11] C. Ciobanu, C.N. Cascaval, D. Rosu, L. Rosu, J. Macromol. Sci. Pure Appl. Chem. 38 (2001) 991–1005.
[12] C.N. Cascaval, C. Ciobanu, D. Rosu, L. Rosu, J. Appl. Polym. Sci. 83 (2002) 138–144.
[13] C.N. Cascaval, D. Rosu, L. Rosu, C. Ciobanu, Polym. Test. 22 (2003) 45–49.
[14] C. Ciobanu, P. Afloarei, C. Barladeanu, C. Culic, Romania Patent 93 590 (1987).
[15] NANOTECH-21, Magurele, PO Box MG-15, Bucharest, Romania.
[16] M. Ulmeanu, A. Serghei, I.N. Mihailescu, P. Budau, M. Enachescu, Appl. Surf. Sci. 165 (2000) 109–115.
[17] C. Wilhelm, A. Rivaton, J.L. Gardette, Polymer 39 (1998) 1223–1232.